Applied Catalysis B: Environmental 209 (2017) 429–436

Contents lists available at ScienceDirect

Applied Catalysis B: Environmental

journal homepage: www.elsevier.com/locate/apcatb

The influence of wall temperature on NO_2 removal and HONO levels released by indoor photocatalytic paints

Adrien Gandolfo[a,*], Louis Rouyer[a], Henri Wortham[a], Sasho Gligorovski[a,b,**]

[a] Aix Marseille Université, CNRS, LCE, UMR 7376, 13331, Marseille, France
[b] State Key Laboratory of Organic Geochemistry, Guangzhou Institute of Geochemistry, Chinese Academy of Sciences, Guangzhou 510 640, China

ARTICLE INFO

Article history:
Received 24 January 2017
Received in revised form 2 March 2017
Accepted 3 March 2017
Available online 6 March 2017

Keywords:
Indoor air
Temperature
Heterogeneous reactions
Nitrogen oxides
Nitrous acid

ABSTRACT

Photocatalytic paints represent a promising remediation technology that has potential to be applied in mechanically ventilated buildings to improve indoor air quality. The photocatalytic paints are typically used to eliminate the gas-phase pollutants, like nitrogen oxides (NO_x) and volatile organic compounds (VOCs).

Here, we demonstrate that indoor photocatalytic paints which contain TiO_2 nanoparticles can substantially reduce the concentrations of nitrogen dioxide (NO_2) at higher surface temperature of the indoor walls. We show that the efficiency of nitrogen dioxide (NO_2) removal increases linearly with the temperature in the range 290–305 K. The geometric uptake coefficients increase from 5.1×10^{-6} at 290 K to 1.5×10^{-5} at 305 K. In the temperature range between 305 and 313 K the removal efficiency of NO_2 remains the same with an average NO_2 uptake coefficient of 1.4×10^{-5}. On the other hand, during the reactions of NO_2 with all the paints (0, 3.5, 5.25 and 7% of TiO_2) a harmful indoor air pollutant, nitrous acid (HONO) is formed, in temperature range between 303 K and 315 K. A maximum HONO value of 6×10^{10} molecules $cm^{-2}\,s^{-1}$ is released by a photocatalytic paint with 7% of TiO_2 (temperature of the walls is 313 K).

A dynamic mass balance model applied to typical indoor environment predicts a steady state mixing ratio between 0 and 4.1 ppb at 296 K and between 2.6 and 10.3 ppb at 305 released upon surface reaction of adsorbed NO_2 with a photocatalytic paint (0, 3.5, 5.25 and 7% of TiO_2) and considering the photolysis process as the most important loss of HONO.

The temperature of the indoor walls is of crucial importance with respect to NO_2 remediation, but at the same time has a strong impact on the formation of harmful intermediates like HONO, which is also a precursor of the OH radicals upon its photolysis.

The photocatalytic paint (7% TiO_2) may contribute up to 57% to the total OH production rate in indoor air, via photolysis of HONO that is released by the paint upon the irradiation, at wall temperature of 305 K.

1. Introduction

In the last 70 years, large efforts have been undertaken to decrease the NO_2 levels in the indoor environments [1]. Yet, the indoor NO_2 levels remain high, falling in the range between 20 ppb and 500 ppb [1–5]. Blondeau et al., 2005 have found a relation between the measured outdoor and indoor concentrations of NO_2 in function of the air exchange rate [6]. Thus, the indoor NO_2 levels vary depending on the proximity of outdoor NO_2 sources [7]. Also, the combustion processes within the indoor environment release high NO_x levels in the indoor air [8–12]. These high NO_2 levels are associated with homes using gas stoves, gas ranges and burning candles or incenses [13]. In the developing countries, cooking and heating the homes with coal, wood, straw, agricultural residues, on open fires and stoves represent an important source of NO_2 in indoor ambiance.

Weschler and Shields [14] indicated that heterogeneous chemistry plays an important role in the indoor environments due to the elevated surface to volume ratios (S/V) (m^{-1}) [15,16] emphasizing the importance of heterogeneous NO_2 reactions. Nazaroff et al.

* Corresponding author at: Aix Marseille Université, CNRS, LCE, UMR 7376, 13331, Marseille, France.
** Corresponding author at: State Key Laboratory of Organic Geochemistry, Guangzhou Institute of Geochemistry, Chinese Academy of Sciences, Guangzhou 510 640, China.
E-mail addresses: adrien.gandolfo@etu.univ-amu.fr (A. Gandolfo), saso.gligorovski@univ-amu.fr, gligorovski@gig-ac.cn (S. Gligorovski).

http://dx.doi.org/10.1016/j.apcatb.2017.03.021
0926-3373/

[17], estimated that indoor surface to volume ratio is up to 300 times higher than outdoors.

Moreover, these NO_2 heterogeneous reactions can be considered as sources of HONO which plays a fundamental role as a source of OH radicals in indoor air, via its photolysis ($\lambda < 400$ nm) during daytime [18]. Despite its importance, sources of HONO remain partially unresolved [19–21] and it was commonly assumed that HONO formation in indoor air is due to heterogeneous processes involving NO_2 and adsorbed water layer on surfaces [22]. Recently, Gómez Alvarez et al. [23] and Bartolomei et al. [24] demonstrated that light-induced heterogeneous processes on indoor surfaces could enhance the conversion of NO_2 into significant amounts of HONO.

NO_2 mixing ratios higher than 100 ppb may impact the human health on a short term exposure [25]. Kim et al. [26] have shown that children exposed to high NO_2 mixing ratios can have respiratory problems. Harwood et al. [27] have shown that long term HONO exposure may modify human DNA. More recent studies have shown that HONO may react with surface deposited nicotine from tobacco smoke, to form nitrosamines (TSNAs) known as third hand smoke (THS) [28].

Photocatalytic paints have been implemented indoors with the aim to eliminate volatile organic compounds (VOC) and nitrogen oxides (NO_x), and maintain surfaces free of bacteria and fungi, among other applications [29,30].

Indeed, photocatalytic paints have been shown to effectively reduce concentrations of nitrogen oxides ($NO_x = NO + NO_2$). Langridge et al. [31] have shown that self-cleaning window glass containing TiO_2 effectively reduces the NO_2 levels but at the same time yields harmful nitrous acid. In contrast, Laufs et al. [32] observed an elimination of HONO on commercial photocatalytic paints used for building facades. Gandolfo et al. [33] have shown that the reactive uptakes of NO_2 on indoor photocatalytic paints increase systematically with the quantity of TiO_2 nanoparticles present in the paint. However, the paint with maximum quantity (7%) of TiO_2 (w/w) released important quantities of NO and HONO. Therefore, further studies are needed to fully understand the HONO formation with respect to the matrix of TiO_2 containing material.

A key parameter which influences the heterogeneous reactions is the light irradiation on the indoor surface [24,34,35]. The light irradiation can also affect the temperature of the surface. The temperature on the irradiated wall in our laboratory falls in the range between 295 K and 312 K in January and April, respectively. To the best of our knowledge only the influence of ambient temperature on NO_2 heterogeneous reactions was studied in the past. El Zein and Bedjanian [36] have shown that the air temperature influences the formation of nitrates and nitrites, rather than the production of NO, HONO and N_2O during the heterogeneous reactions of NO_2 with Al_2O_3 surface [37].

Here, we investigate the influence of the wall's surface temperature on the photocatalytic activity of indoor paints towards NO_x and HONO levels in a flow tube photoreactor simultaneously coupled to a Long Path Absorption (LOPAP) and NO_x analysers for online measurements of HONO and ($NO + NO_2$), respectively.

This study demonstrates that, depending on the wall temperature, as well as the quantity of TiO_2 nanoparticles, indoor photocatalytic paints can be involved in NO_2 removal process and/or in renoxification process to form high quantities of NO and HONO.

2. Materials and methods

The photocatalytic paints were produced by our industrial partner ALLIOS. The paints are prepared by a well-established procedure which was already detailed elsewhere [33]. Photocatalytic paints containing 3.5, 5.25 and 7% of photocatalytic active TiO_2 nanoparticles (w/w), were investigated.

The prepared paint was then applied on one side of glass plates with dimensions 29 cm × 1.9 cm (length × width) and inserted upward oriented into the flow tube photo-reactor.

The TiO_2 nanoparticles replace the $CaCO_3$ which alters the density of the paint and it affects the pH of the paint. Prior to experiments, we have measured the pH of 4 different paints (0, 3.5, 5.25, 7% of TiO_2), using a protocol adapted from a well-established procedure of pH measurements in soil samples (ISO 10390 2005). 250 mg of a dry paint was mixed with 25 ml of distilled water (MilliQ). The solution was agitated during 5 min and then let 1 h in a dark. This procedure was repeated two times. To get rid of the remaining residues the solution was filtered by a syringe filter. The pH of this solution during the agitation was measured by a pH meter (Consort multi-parameters C3050).

The photocatalyst (TiO_2) which is introduced in the paint is sensitive to the UV light (300 nm < λ < 390 nm). The replacement of $CaCO_3$ with the slurry alters the density and may influence the paint stability. For this reason, the maximum allowed quantity of TiO_2 (w/w) in the paint is 7%.

2.1. The flow tube reactor

The flow tube photo-reactor is depicted in Fig. 1 [33]. The flow tube is constituted of a cylindrical borosilicate glass tube ($V = 131\ cm^3$) inserted into a double-wall reactor with connections to a thermostatic bath which allowed operation at different temperatures. The gaseous NO_2 is introduced into the reactor via a movable injector equipped with a fritted end. While varying the position of the injector inside the reactor we control the contact time between the gaseous NO_2 and the painted surface which allows to elucidate the kinetics. Each position of the injector is maintained for about 30 min to attain a steady state NO_2 concentration. The total duration of each experiment for the four different injector position is 4 h.

The flow tube reactor was thermostated using a circulating water bath through the outer jacket (Lauda RC6 refrigerated bath with RCS thermostat, temperature accuracy = ±0.02 K at 263 K, which also permitted to control the temperature on the painted surface. The thermostated bath is started 2 h prior to experiments which allows stable surface temperature conditions.

A certified mixture of NO_2 (100 ppm) in Helium (Linde gas) was connected to a mixing loop fed by synthetic air (Linde gas 5.0) to allow two successive dilutions. For the first dilution, a NO_2 flux of 10 ml min^{-1} (0–20 ml min^{-1} Brooks SLA Series mass flow controller; accuracy, ±1%) is incorporated in the 490 ml min^{-1} synthetic air flow (0–500 ml min^{-1} Brooks SLA Series mass flow controller; accuracy, ±1%). Then a flow of 20 ml min^{-1} of this mixture was introduced through the movable injector (0–20 ml min^{-1} Brooks SLA Series mass flow controller; accuracy, ±1%) into the

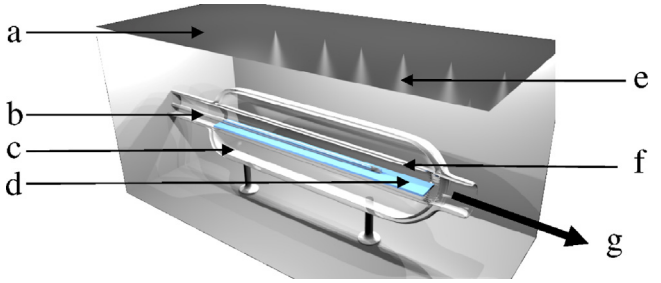

Fig. 1. 3D-skatch of (a) stainless steel box, (b) mobile injector, (c) double wall thermostated glass envelope, (d) glass plate covered with the paint, (e) UV lamps (f) the flow tube photo-reactor, and (g) exit of the flow gas to the NO_x and HONO analyzers.

reactor. A sheath flow of 980 ml min^{-1} (Linde gas 5.0, flow controller Brooks SLA 0–1 l min^{-1}) was also introduced in the reactor to obtain 40 ppb of NO_2 typical for indoor environment. The flow tube photo-reactor is designed to operate under gas-phase laminar flow conditions. The temperature of the gas is measured at the end of the reactor with the hygrometer "Hygrolog NT2" (Rotronic) with a "HygroClip SC04" probe. Considering that gas flow in the reactor is 1 l min^{-1} implies that it remains less than 8 s in the reactor. Thus, the temperature remains constant while the gas drifts through the reactor.

The sheath flow was fed to a bubbler before its introduction in the reactor. Humidity was accordingly fixed by separating the sheath flow in two fluxes controlled by needle valves, one of dry air flow and the other humidified by bubbling through deionised water. A mixing of these two flows at different ratios generated a carrier gas at controlled relative humidity. Downstream of this device, a hygrometer "Hygrolog NT2" (Rotronic) with a "HygroClip SC04" probe measured on-line the resulting relative humidity. For these experiments the relative humidity was set at 40% with ±1.5% accuracy.

The temperature of the surface was measured by a multimeter DM 220 equipped with a k-type thermocouple connector (228 and 1023 K, ±3% accuracy). Hence, the incertitude in the temperature range between 288 K and 318 K is 0.5 K and 1.4 K, respectively. The surface temperature measurements were assured making a double check with a non-contact digital laser infrared thermometer (Laserliner, Thermospot, 253 and 623 K, ±2% accuracy). Thus, for these measurements the incertitude in the temperature range between 288 K and 318 K is 0.3 K and 0.9 K, respectively. This study was performed at three different temperatures, 296 K, 305 K and 313 K for all the paints.

The flow tube photo-reactor is surrounded by six UV lamps (Philips TL-D 18 W, 340–400 nm, λ_{max} = 368 nm, length = 60 cm). The reactor and the lamps are placed in a stainless steel box. For this study we considered the integrated irradiance of two lamps in the wavelength region between 340 nm and 400 nm with total intensity of 8.5 W m^{-2} which corresponds to the intensity (9 W m^{-2}) of integrated irradiance in the same wavelength region of direct sunlight irradiating the indoor painted walls [24]. The UV light emitted by the lamps coincide with the UV fraction of the sunlight which penetrates indoors allowing to conduct the experiments under relevant conditions [38].

2.2. NO_x and HONO measurements

NO_x, NO_2 and NO concentrations were simultaneously measured by a chemiluminescence instrument (Eco Physics, model CLD 88p) hyphenated to a photolytic (metal halide lamp) converter (Eco Physics, model PLC 860). The advantage of the photolytic process is that the sample gas passes through a cell where it is exposed to light (320 nm < λ < 400 nm) from a metal halide lamp. This causes the NO_2 to be selectively converted to NO with negligible interference to other gases [39,40]. The NO_x analyzer is very sensitive [41] with a detection limit of 110 ppt and a time resolution of 1 s.

The gas phase HONO concentration was measured using a LOng Path Absorption Photometer (LOPAP, QUMA). A detailed description of its operation principle and procedure can be found in the literature [42–44]. Briefly, HONO is chemically sampled in an external sampling unit in an aqueous solution and is measured photometrically in long-path absorption in the visible after conversion into an azodye (550 nm) in the measuring instrument. Special Teflon tubing (Teflon AF2400) serves as a long-path absorption cell by which light can be transferred in total reflection caused by the low refractive index of the material. During all the experiments the detection limit was smaller than 3 ppt with a total accuracy of ±10% with an actual time response of about 5 min under the operation conditions applied (gas flow and pump flow of 1 l min^{-1} and 20 μL min^{-1}, respectively) and a time resolution of 15 s.

3. Results and discussion

3.1. Reaction mechanism of NO_2 on TiO_2 photocatalytic paints

Conduction-band electrons (e^-_{cb}) and valence-band holes (h^+_{vb}) are generated when UV light at λ < 390 nm dissociate the photocatalyst (TiO_2) (R1).

$$TiO_2 + h\nu \rightarrow e^-_{cb} + h^+_{vb} \quad (R1)$$

Molecular oxygen acts as electron acceptor leading to the formation of superoxide (O_2^-) radicals, as follows:

$$e^-_{cb} + O_2 \rightarrow O_2^- \quad (R2)$$

Water molecules and hydroxyl anions adsorbed on the photocatalytic paint (TiO_2) surface, act as electron donors, leading to the formation of hydroxyl radicals (OH) on the surface of the paints:

$$h^+_{vb} + H_2O \rightarrow OH + H^+ \quad (R3)$$

When NO_2 is adsorbed onto TiO_2 semiconductor surface, the surface reaction with hydroxyl radical occurs, according to Langmuir–Hinshelwood kinetic mechanism.

$$NO_2 + OH \rightarrow HNO_3, \qquad HNO_3 \rightleftharpoons NO_3^- + H^+, \quad pK_a \approx -2 \quad (R4)$$

Nitric acid (HNO_3), produced via (R4), is considered as a permanent sink of NO_x.

$$NO_2 + O_2^-(+H^+) \rightarrow NO_2^-(HONO) + O_2 \quad (R5)$$

Finally the following catalytic net reaction is obtained:

$$2NO_2 + H_2O \xrightarrow{+h\nu,\ TiO_2} HONO + HNO_3 \quad (R6)$$

The photolysis of HONO is the most important source of OH radicals in the indoor air [18,45].

Pioneering theoretical studies performed by McGrath and Rowland and Sumathi and Peyerimhoff [46–48] suggested that there could be up to three energetically feasible conformers of peroxynitrous acid (HOONO) formed via surface reaction (R7).

$$NO_2 + OH \rightarrow HOONO \quad (R7)$$

Fundamental molecular insights gained from theoretical calculations were confirmed by the experimental observations conducted by Nizkorodov and Wennberg using vibrational overtone photodissociation spectroscopy [49]. The formation of the most stable cis–cis conformer of HOONO was confirmed [49]. Matheu and Green suggested an upper limit to the formation rate of HOONO as 20% of that of HNO_3. It is highly plausible that HOONO has sufficiently long life-time to partition to the gas-phase [50]. Although minor, the reaction channel given by (R7) could be important from air quality point of view since HOONO easily dissociates in wavelength region available indoors to form NO_2 and OH [51]. In addition to the photolysis of HONO, the photolysis of HOONO could be an additional source of OH radicals in presence of photocatalytic paints.

3.2. Reactive uptakes of NO_2

In this study, the reactive uptakes of NO_2 (γ_{NO_2}) were investigated in function of different quantities 0, 3.5, 5.25 and 7% of TiO_2 nanoparticles at 296 K, 305 K and 313 K (Fig. 2).

γ_{NO_2} is the dimensionless uptake coefficient of NO_2 which defines the reaction probability of gas-phase NO_2 on the paint surface. The reactive uptakes of NO_2 can be estimated as a function

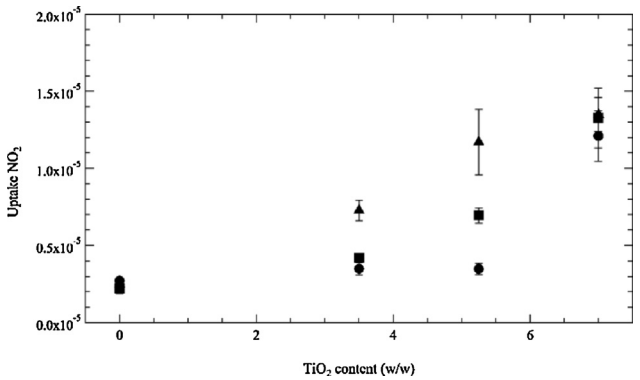

Fig. 2. NO_2 uptake coefficients as a function of the TiO_2 nanoparticles content at NO_2 mixing ratio of 40 ppb, 8.5 W m^{-2} UVA and RH of 40% at different temperatures on the surface of the paint: (●) 296 K; (■) 305 K; (▲) 313 K. The error bars are derived from the uncertainties associated to the estimation of the uptake coefficients.

of the gas phase-painted surface exposure time. For this study the reactive uptake of NO_2 was estimated as follows:

$$\gamma_{NO_2} = \frac{4 \times k_{NO_2}}{\upsilon_{NO_2} \times A} \quad (1)$$

where k_{NO_2} is the pseudo first order rate constant for the reaction between NO_2 and the surface, υ_{NO_2} is the average molecular speed of NO_2, and A describes the geometry of the reactor as a ratio between the reactive surface and the volume of the reactor.

Gandolfo et al. [33] have shown that γ_{NO_2} measured at ambient temperature (296 K) increased with the quantity of introduced TiO_2 nanoparticles in the paints under UV irradiation at 20 W m^{-2}. Fig. 2 shows that the reactive uptakes of NO_2 on white wall paints in absence of TiO_2 are not influenced by the temperature. On the other hand, the reactive uptakes of NO_2 on photocatalytic paints embedded with TiO_2 nanoparticles, increase with the temperature, under UV light irradiation at 8.5 W m^{-2}. This effect is most pronounced for the paints containing 5.25% of TiO_2 nanoparticles where the difference between the γ_{NO_2} at 296 K, 305 K and 313 K is noticeable. Quite intriguing is the behaviour of the photocatalytic paint with 7% of TiO_2. It seems that γ_{NO_2} reaches the maximum value of about 1.4×10^{-5} and it does not further increases with rise of the temperature. The reason for this could be that the reactive uptakes on paint with 7% of TiO_2 reach the plateau and further increase of the temperature would not have any impact on γ_{NO_2}. The adsorption of gaseous NO_2 on the surface of the photocatalytic paints depends on adsorption site and binding energy [52]. Gaseous NO_2 molecules tend to adsorb on sites with higher binding energies. Theoretical studies [53] indicate that the increase of temperature reduces the binding energy due to the reduction of the electron spatial probability density at higher temperatures. This could be the reason that the adsorption of NO_2 on a paint with 5.25% and 7% of TiO_2 becomes limited as the temperature increases. Consequently, the reaction of adsorbed NO_2 with the TiO_2 (5.25 and 7% w/w) semiconductor surface becomes limited, as well (Fig. 2).

Most importantly, the reactive uptake of NO_2 at 305 K is higher for the paint with 5.25% of TiO_2 than the paint with 3.5% and the paint in absence of TiO_2. This was not the case at ambient temperature (296 K) because the same uptakes were observed on the paints with 3.5% of TiO_2 and 0% of TiO_2 which was ascribed to the scavenging of OH radicals formed by the reaction of water with the valence band hole [33]. However, our measurements of the temperature on the walls irradiated with sunlight irradiation, indicate that the wall surface temperature could reach up to 313 K. The higher uptakes of NO_2 at 305 K and 313 K for the paint containing 5.25% of TiO_2 indicates that these photocatalytic paints are more efficient towards NO_2 elimination and thus more suitable for indoor air remediation.

3.3. Formation of NO and HONO

While the photocatalytic paint efficiently eliminates gas-phase NO_2, it gives rise to the gaseous HONO as shown in Fig. 3.

The quantity of TiO_2 nanoparticles embedded in the paint influences the formation of HONO [33]. In fact, only the paint containing 7% of TiO_2 released HONO under higher light intensity (20 W m^{-2}; 340 nm < λ < 400 nm) at room temperature [33]. Fig. 3 shows the same behaviour (black circles) under moderate (more realistic) [24] light irradiation of 8.5 W m^{-2}.

The alkalinity of the paints may influence the formation of HONO considering its acid character (p K_a (HONO) = 3.16 at 298 K) [54]. Following a well-established experimental procedure, as described in Section 2, we measured the pH values of the studied paints as follows: (8.9 ± 0.06), (8.6 ± 0.02), (8.2 ± 0.07), and (8.2 ± 0.03) which correspond to the paints with 0, 3.5, 5.25, 7% of TiO_2 nanoparticles, respectively. The measured pH values indicate that the photocatalytic paints are slightly less alkaline compared to the non-photocatalytic paint (0% of TiO_2). The concentrations of the measured H^+ ions were 1.9, 5.2, and 4.5 times higher than the [H^+] of the non-photocatalytic paint.

The non-linear dependence of HONO on the TiO_2 nanoparticle content depicted in Fig. 3 observed at different temperatures indicates that indeed the reaction of adsorbed NO with the photocatalytically produced OH radicals (R8) is most probably the principal source of HONO as suggested earlier [33].

$$NO(ads) + OH(ads) \xrightarrow{TiO_2} HONO \quad (R8)$$

An increase of the surface temperature at 305 K induces HONO emission in the order of 2×10^{10} molecules cm^{-2} s^{-1}, by the paints containing 3.5 and 5.25% of TiO_2. At 305 K, even the non-photocatalytic paint releases a HONO flux of about 2×10^{10} molecules cm^{-2} s^{-1}. These observations indicate that the pH value does not affect the HONO emissions at higher surface temperatures.

Yet, the paint with 7% of TiO_2 ehxibits different behaviour compared to the other paints, producing two times higher HONO level at 305 K (Fig. 3). A further increase of the temperature (313 K) only slightly influences the formation of HONO. A maximum HONO formation of 6×10^{10} molecules cm^{-2} s^{-1} is observed for the paint containing 7% of TiO_2 at 313 K.

To understand the HONO production by photocatalytic paints at higher surface temperatures we suggest the following mechanism.

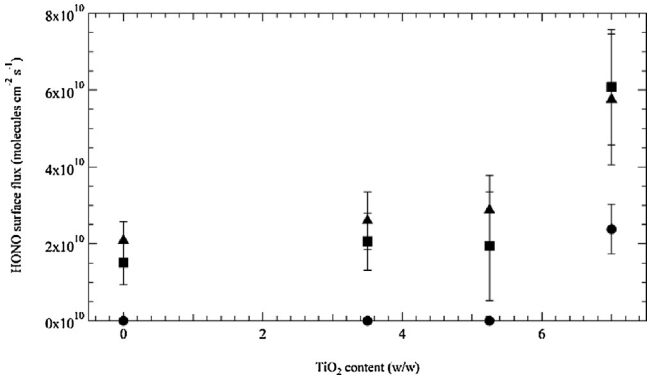

Fig. 3. HONO formation on photocatalytic paints with 0, 3.5, 5.25 and 7% of TiO_2 nanoparticles at (●) 296 K; (■) 305 K; (▲) 313 K. NO_2 mixing ratio is 40 ppb and RH is 40%. Error bars indicate the standard deviation from four independent measurements.

The gaseous NO_2 partition with the paint surface:

$$NO_{2(g)} \rightleftarrows NO_{2(ads)} \quad (R9)$$

The adsorbed NO_2 on the surface of the photocatalytic paints reacts with superoxide (O_2^-) ion which emerges from (R2).

$$NO_{2(ads)} + O_2^- \rightarrow NO_2^-{}_{(ads)} \quad (R10)$$

The nitrites dissolve in the adsorbed water layer on the paint surface, undergoing the reversible acid-base reaction, as follows:

$$NO_{2(ads)}^- + H_{(aq)}^+ \rightleftarrows HNO_{2(aq)} \quad (R11)$$

HNO_2 represents a nitrous acid in the aqueous phase (aq), which reversibly dissociate into H^+ and NO_2^- ions.

Alternatively, aqueous nitrous acid partition to the gas phase

$$HNO_{2(aq)} \rightleftarrows HONO_{(g)} \quad (R12)$$

There is an equilibrium between $HNO_{2(aq)}$ and $HONO_{(g)}$ designated as HONO*. The equilibrium concentration of [HONO]* is strongly dependent on pH and the concentration of NO_2^-.

When [HONO]* is higher than the gas phase concentration of [HONO], nitrous acid is released in the gas phase. Contrary, when [HONO]* is lower than the concentration of [HONO] in the gas phase, nitrous acid is deposited on the surface. Then, the equilibrium concentraion of [HONO]* is given as follows:

$$[HONO]^* = \frac{[HNO_2] + [NO_2^-]}{H^*} \quad (2)$$

where H^* represents the effective Henry's law constant and where the sum of $[HNO_2]$ and $[NO_2^-]$ represents the total nitrite concentration often denoted in the literature as [N(III)] [55].

$$H^* = H_{HNO_2}\left(\frac{1 + K_a}{[H^+]}\right) \quad (3)$$

whereas H_{HNO_2} represents the henry's law coeficient of HNO_2 and K_a is the acid dissociation constant of nitrous acid. The Henry's law constants of nitrous acid at four different temperatures in the range between 273 and 303 K are given in the literature. For example, the H_{HNO_2} is 60 M atm^{-1} at 295 K and 38 mol atm^{-1} at 303 K, which could possibly be the reason for the higher gas-phase HONO concentration observed at 303 K then at 295 K.

Thus, 1) the evaporation of the water layer from the paint surface at higher temperatures induces higher concentration of $HNO_{2(aq)}$ which promotes the release of HONO in the gas phase and 2) the increase of the surface temperature diminishes the H^* values implying an increase of [HONO]*, thus, HONO emission in the gas phase.

The yields of conversions of the two products NO and HONO formed during the heterogeneous reactions of NO_2 with the photocatalytic paints as a function of the temperature, are presented in Fig. 4.

Fig. 4 shows that the HONO yield which is estimated as a ratio $\Delta HONO/\Delta NO_2$ increases with the temperature indicating that the increase of the HONO formation is bigger than the increase of the NO_2 loss.

The formation of NO yields increases with the temperature from 0% at 290 K up to 30% at 305 K for the paint containing 7% of TiO_2. Surprisingly there is no formation of NO at 313 K. HONO is also formed with lower yields (ca. 4%) at ambient temperature (295 K) and increases in a nonlinear way up to 17% at 313 K.

The sum of both NO and HONO yields is lower than 50% at elevated wall's temperature suggesting that the rest of NO_2 is converted to adsorbed nitric acid/nitrate (HNO_3/NO_3^-) and to a lesser extent the peroxynitrous acid (HOONO).

It is important to note that these NO_2/HONO and NO_2/NO conversion yields are observed under UV-A light (325 nm < λ < 400 nm) irradiation of the photocatalytic paint with light intensity of 8.5 W m^{-2} typical for indoor environment [38].

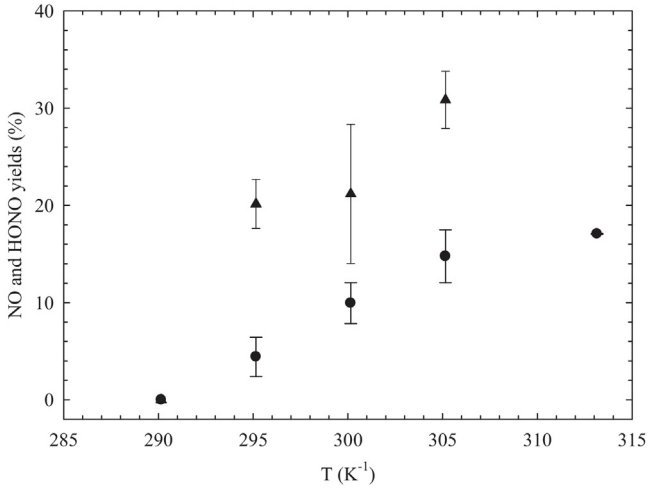

Fig. 4. (●) HONO and (▲) NO yields from conversion of NO_2 (40 ppb) on a photocatalytic paint with 7% of TiO_2 nanoparticles as a function of the temperature (290–313 K) at 40% RH under irradiation with 8.8 W m^{-2} UV light. Error bars indicate the standard deviation from four independent measurements.

3.4. Implications for typical indoor environments

HONO is an emerging indoor air pollutant [19] which exhibits adverse health effects. The release of HONO by the walls can strongly influence the indoor air quality. Namely, HONO easily dissociates (λ < 400 nm) in the indoor environment [18] and produces highly reactive hydroxyl radicals which determine the oxidative capacity of the indoor atmosphere. The results from this study indicate that the wall's temperature strongly influence the HONO release from the photocatalytic paints which in turn affects the oxidative capacity in the indoor atmospheres.

From the experimental results, we estimate the indoor air implications of the photocatalytic paints by dynamic mass balance model.

Assuming an average sized room that is 2.5 m high, 5 m wide and 4 m long; hence a room with a total volume of 50 m^3 and to simulate more realistic conditions, this model assumes that only 4 m^2 is irradiated with direct sunlight of 8.5 W m^{-2} (340 < λ < 400 nm) yielding a HONO emission rates (Table 1) upon irradiation of all our paints at wall temperatures of 296 K and 305 K, respectively. Namely, after detailed observations of the sunlight irradiation of the indoors walls in a real southwest oriented room we reduced the irradiated surface ca. 30% in comparison to the assumed irradiated surface in the previous study [33].

Considering an average air-exchange rate of 0.56 h^{-1} [56], we can estimate the concentration of HONO produced by the reference paint and the photocatalytic paints. The photolysis frequency of HONO was estimated assuming direct light irradiation as $J(HONO) = 1.7 \times 10^{-4}$ s^{-1}.

For details about the dynamic mass balance model applied in indoor environment see Gandolfo et al. [33].

Assuming that only one fifth of the volume of the room is directly irradiated with UVA irradiation (340 nm < λ < 400 nm) we obtain the HONO mixing ratios in function of time released by the photocatalytic paints which contain 3.5, 5.25 and 7% of TiO_2 at different wall's temperatures (Fig. 5). For comparison purpose the HONO emission by non-photocatalytic paint is also given.

At 296 K only the photocatalytic paint with 7% of TiO_2 produces 4 ppb of steady state HONO. But, the increase of wall surface temperature leads to enhanced HONO formation by all the paints. A steady state HONO of 2.6, 3.4, 3.3 and 10.3 ppb is reached after 3 h at 305 K for the paints containing 0, 3.5, 5.25 and 7%, respectively. This HONO value is higher (under similar assumed conditions) than the

Table 1
Emission surface fluxes of HONO measured in the flow tube reactor and HONO emission rates normalized to 4 m^2 of indoor wall covered with paints containing 0, 3.5, 5.25, 7% of TiO_2 at 296 K and 305 K. Error bars represent 1σ precision.

TiO_2 content (%)	Surface temperature			
	296 K		305 K	
	Surface emission flux (molecules cm^{-2} s^{-1})	Emission rates (mg h^{-1})	Surface emission flux (molecules cm^{-2} s^{-1})	Emission rates (mg h^{-1})
0	0	0	$(1.5 \pm 0.6) \times 10^{10}$	0.17 ± 0.06
3.5	0	0	$(2.1 \pm 0.7) \times 10^{10}$	0.23 ± 0.08
5.25	0	0	$(1.9 \pm 1.4) \times 10^{10}$	0.22 ± 0.16
7	$(2.4 \pm 0.7) \times 10^{10}$	0.3 ± 0.07	$(6.1 \pm 1.5) \times 10^{10}$	0.68 ± 0.17

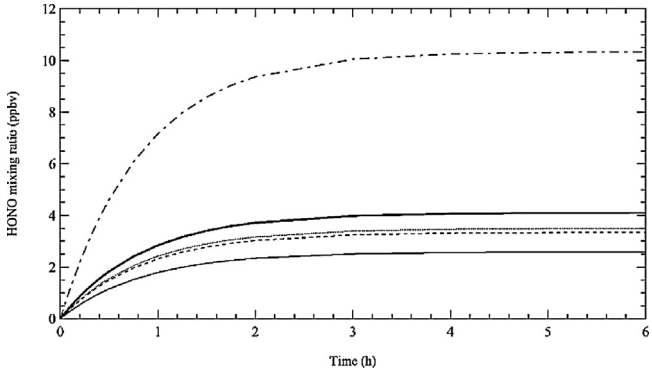

Fig. 5. The estimated mixing ratios of HONO emitted by the reference paint and photocatalytic paints containing 3.5, 5.25 and 7% of TiO_2 (w/w) under an irradiation of 8.5 W m^{-2}, at 40 ppb of NO_2 and 40% RH in function of time. Bold solid black line corresponds to a photocatalytic paint with 7% of TiO_2 at 296 K; solid black line, dotted line, dashed line, and dash-dotted line correspond to HONO mixing ratios emitted by paints with 0%, 3.5%, 5.25% and 7% of TiO_2 at 305 K.

Table 2
List of alkenes typical for indoor environment including the parameters used for the model calculations.

Alkene	Typical indoor concentration [58] (molecules cm^{-3})	Ozonolysis rate constant [59,60] (molecules cm^{-3} s^{-1})	OH yield [14]
D-Limonene	7.25×10^{10}	2.04×10^{-16}	0.86
α-Terpinene	7.50×10^{8}	8.40×10^{-15}	0.91
2-Methyl-2-butene	5.75×10^{9}	4.00×10^{-16}	0.89
α-Pinene	1.08×10^{10}	8.40×10^{-17}	0.85
Trans-2-buetene	5.50×10^{9}	2.12×10^{-16}	0.64

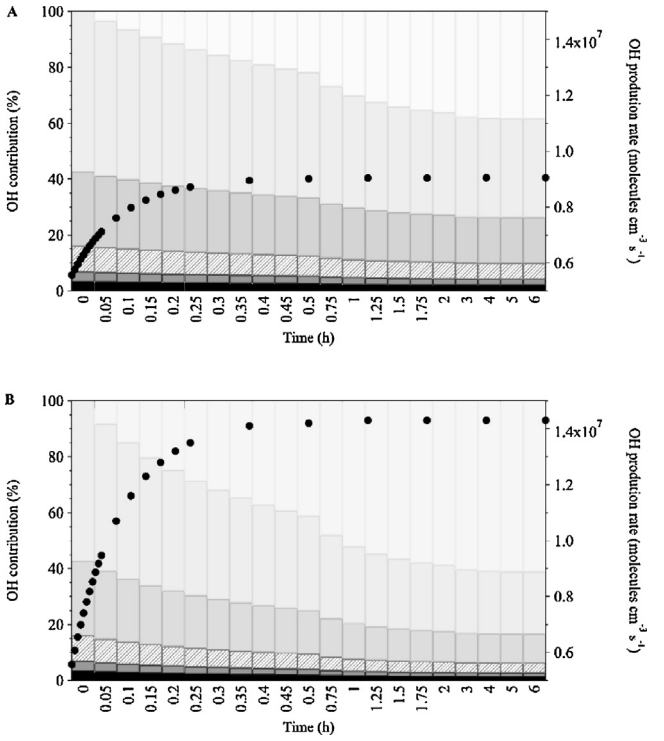

Fig. 6. (Left axis) The estimated OH contribution in the modelled room by HONO photolysis (very light gray), ozonolysis of D-limonene (light gray), ozonolysis of α-terpinene (gray), ozonolysis of 2-methyl-2-butene (mocked gray), ozonolysis of α-pinene (dark gray), ozonolysis of trans-2-butene (dark); (right axis) OH production rate by photocatalytic paint with 7% of TiO_2 at (A) 296 K and (B) 305 K.

HONO (1.6 ppb) released by non-photocatalytic paint, lacquer and glass altogether [23] demonstrating that certain precautions should be taken while optimizing the photocatalytic materials aimed for air purification in the indoor settings.

Considering that HONO is the major source of OH radicals in indoor air [18,45,57], the high quantities of HONO released by the non-photocatalytic and photocatalytic paints at elevated wall temperature, may induce serious repercussion on indoor air quality. In order to demonstrate the importance of HONO within indoor environment, we compared (Fig. 6) the contributions of HONO photolysis and the ozonolysis of alkenes, to the production of OH radicals in indoor air. We considered that only 20% of the room is irradiated with direct sunlight and only in this volume occurs the photolysis of HONO.

Regarding the ozonolysis of the alkenes, we have chosen 5 representative alkenes (Table 2) which exhibit highest OH production rate due to their average concentrations in indoor air [58], the reaction rates towards ozone [59,60], and their yields of OH formation.

For the comparison of the OH production rates depicted in Fig. 6 we have chosen an average ozone mixing ratio of 10 ppb considering that the typical background ozone mixing ratios in an urban environment range between 35 and 40 ppb [61]. This assumption is reasonable knowing that indoor ozone levels vary between 0.2 and 0.7 times of the outdoor levels [62] strongly depending on the air exchange rates. Regarding the recently developed low-energy buildings with lower air exchange rates using the photocatalytic paints as a remediation technology, the indoor ozone levels would be rather about 0.2 times of the outdoor background ozone concentration.

Fig. 6A shows the production of OH radicals in indoor air by photolysis of steady state HONO (Fig. 5) released by photocatalytic paint (7% of TiO_2) at 296 K, and by ozonolysis of five highly reactive alkenes in indoor air. At time t_0 the indoor wall begins to be irradiated initiating the production of OH radicals by photolysis of HONO which is generated by the irradiated photocatalytic paint. After 30 min the contribution of HONO photolysis to the production of OH radicals is 22% and it reaches the plateau (38%) after 1 h and 30 min. At this moment the photolysis of HONO and ozonolysis of D-limonene represent the major source of OH radicals. The sum of both sources contribute ca. 75% to the production of OH radicals. The other 25% are attributed to the ozonolysis of α-terpinene

and 2-methyl-2-butene. The reactions of ozone with α-pinene and trans-2-butene contribute only 5% to the total OH production.

At 305 K the photolysis of HONO emerged from the photocatalytic paint (7% of TiO_2) becomes dominant source of OH radicals (Fig. 6B). Only for a very short period, at $t = 3$ min the ozonolysis of alkenes is the major source of OH radicals (92%). Then, the situation rapidly changes and at $t = 30$ min the photolysis of HONO contributes with 41% to the OH production while after 1 h and 30 min, photolysis of HONO contributes with 57% to the total production of OH radicals. For example, at $t = 30$ min, the photolysis of HONO is ca. 30% bigger OH source than the ozonolysis of D-limonene and about 300% more important OH source than the ozonolysis of α-terpinene. The ozonolysis of other alkenes contributes only 9% to the total OH production. At $t = 90$ min, the ozonolysis of D-limonene contributes with only 25% to the total OH production.

Intriguingly, the non-photocatalytic paint generates HONO at 305 K, as well. The emerged model results suggest that at $t = 30$ min the photolysis of HONO generated by the non-photocatalytic paint contributes with 15% to the total OH production against 49% and 22% ascribed to the ozonolysis of D-limonene and α-terpinene, respectively. At $t = 90$ min the contribution of HONO (released by non-photocatalytic paint) photolysis to the OH production reaches maximum 25% at 305 K. Thus, the non-photocatalytic paint can be considered as an important source of OH radicals in indoor air. The performed model results indicate that the conventional non-photocatalytic paint exhibits an OH production rate of 2×10^6 molecules cm^{-3} s^{-1}.

On the other hand, the total OH production rates by the photocatalytic paints and the ozonolysis of the five considered alkenes, at $t = 30$ min, is 9×10^6 molecules cm^{-3} and 1.4×10^7 molecules cm^{-3}, at 296 K and 305 K, respectively. These results indicate that an increase of only 9 K leads to an increase of 50% of total OH production rate due to the photolysis of HONO emerged from the photocatalytic paints. The total OH production rate (1.4×10^7 molecules cm^{-3}) in this study represented by the photolysis of HONO formed by photocatalytic paint (7% of TiO_2) at 305 K and ozonolysis of five representative alkenes falls in the same order as the reported OH production rate (3×10^7 molecules cm^{-3} s^{-1}) in polluted urban area in London [63] or in rural environment at Pennsylvania [64].

4. Concluding remarks

The temperature on the indoor walls is an important parameter controlled by heating, air exchange rate and outdoor climatic conditions such as sunlight irradiation of the indoor environment. Our measurements indicate that the indoor wall's temperature varies over a broad range starting from 290 K during the winter in absence of sunlight, up to 313 K during the spring period under direct sunlight irradiation.

In this study we demonstrate that the changes of temperature on the indoor walls alters the remediation activity of photocatalytic paints towards NO_2. The increase of wall's temperature leads to enhanced NO_2 uptakes from 7.5×10^{-6} at 290 K to 1.4×10^{-5} at 305 K with a saturation uptake efficiency in the temperature range between 305 and 313 K with an average NO_2 uptake coefficient of 1.3×10^{-5}. A comprehensive knowledge about the uptake coefficients of NO_2 on indoor surfaces is crucial for a rigorous kinetic representation of the heterogeneous reactions in modelling studies [19].

Unfortunately, the increase of wall's temperature results in elevated production of harmful gas-phase by-products such as HONO in indoor air. Namely, the photocatalytic paints with 3.5 and 5.25% of TiO_2 that are not supposed to release HONO at ambient temperature [33] represent an important source of HONO at 305 K with surface fluxes of $(2.1 \pm 0.7) \times 10^{10}$ molecules cm^{-2} s^{-1} and $(1.9 \pm 1.4) \times 10^{10}$ molecules cm^{-2} s^{-1}, respectively. At 305 K, the paint with 7% of TiO_2 exhibits temperature saturated NO_2 to HONO conversion with an average HONO surface flux of 6×10^{10} molecules cm^{-2} s^{-1}.

A dynamic mass balance model was used to assess the evolution of HONO in function of time in a real-life indoor environment.

The emerged modelling results suggest that surface temperature strongly influences the heterogeneous HONO formation induced by the non-photocatalytic and photocatalytic paints which in turn impacts the oxidative capacity of indoor atmosphere via HONO photolysis.

The conventional non-photocatalytic paint that does not release HONO at ambient temperature, it becomes an important HONO source at 305 K with a contribution of 25% to the total OH production rate. The contribution to the total OH production rate in indoor environment becomes even more important for the photocatalytic paints containing the TiO_2 nanoparticles. For example, the paint with 7% of TiO_2 contributes 60% to the total OH production rate via photolysis of HONO that is released by this paint.

The model results from this study contribute to rationalize unresolved discrepancy between the measured and modelled HONO and OH values in the indoor environments [57].

Acknowledgement

This work is a contribution to the LABEX SERENADE (n° ANR-11-LABX-0064) funded by the «Investissements d'Avenir», French Government program of the French National Research Agency (ANR) through the A*Midex project (No. ANR-11-IDEX-0001-02).

References

[1] C.J. Weschler, Changes in indoor pollutants since the 1950s, Atmos. Environ. 43 (2009) 153–169.
[2] P.N. Breysse, T.J. Buckley, D. Williams, C.M. Beck, S.J. Jo, B. Merriman, S. Kanchanaraksa, L.J. Swartz, K.A. Callahan, A.M. Butz, C.S. Rand, G.B. Diette, J.A. Krishnan, A.M. Moseley, J. Curtin-Brosnan, N.B. Durkin, P.A. Eggleston, Indoor exposures to air pollutants and allergens in the homes of asthmatic children in inner-city Baltimore, Environ. Res. 98 (2005) 167–176.
[3] K. Lee, J. Xue, A.S. Geyh, H. Ozkaynak, B.P. Leaderer, C.J. Weschler, J.D. Spengler, Nitrous acid, nitrogen dioxide, and ozone concentrations in residential environments, Environ. Health Perspect. 110 (2002) 145–149.
[4] C. Monn, Exposure assessment of air pollutants: a review on spatial heterogeneity and indoor/outdoor/personal exposure to suspended particulate matter, nitrogen dioxide and ozone, Atmos. Environ. 35 (2001) 1–32.
[5] G. Gallelli, P. Orlando, F. Perdelli, D. Panatto, Factors affecting individual exposure to NO_2 in Genoa (northern Italy), Sci. Total Environ. 287 (2002) 31–36.
[6] P. Blondeau, V. Iordache, O. Poupard, D. Genin, F. Allard, Relationship between outdoor and indoor air quality in eight French schools, Indoor Air 15 (2005) 2–12.
[7] G. Emenius, G. Pershagen, N. Berglind, H.-J. Kwon, M. Lewné, S.L. Nordvall, M. Wickman, NO_2, as a marker of air pollution, and recurrent wheezing in children: a nested case-control study within the BAMSE birth cohort, Occup. Environ. Med. 60 (2015) 876–881.
[8] D. Ross, Continuous and passive monitoring of nitrogen dioxide in UK homes, Environ. Technol. 17 (1996) 147–155.
[9] N. Bernard, M. Saintot, C. Astre, M. Gerber, Personal exposure to nitrogen dioxide pollution and effect on plasma antioxidants, Arch. Environ. Health Int. J. 53 (1998) 122–128.
[10] J. Cyrys, J. Heinrich, K. Richter, G. Wölke, H.E. Wichmann, Sources and concentrations of indoor nitrogen dioxide in Hamburg (west Germany) and Erfurt (east Germany), Sci. Total Environ. 250 (2000) 51–62.
[11] S.J. Dutton, M.P. Hannigan, S.L. Miller, Indoor pollutant levels from the use of unvented natural gas fireplaces in Boulder, Colorado, J. Air Waste Manag. Assoc. 51 (2001) 1654–1661.
[12] Ó. García-Algar, M. Zapater, C. Figueroa, O. Vall, X. Basagaña, J. Sunyer, A. Freixa, X. Guardino, S. Pichini, Sources and concentrations of indoor nitrogen dioxide in Barcelona, Spain, J. Air Waste Manage. Assoc. 53 (2003) 1312–1317.
[13] V. Bartolomei, E. Gomez Alvarez, J. Wittmer, S. Tlili, R. Strekowski, B. Temime-Roussel, E. Quivet, H. Wortham, C. Zetzsch, J. Kleffmann, S. Gligorovski, Combustion processes as a source of high levels of indoor hydroxyl radicals through the photolysis of nitrous acid, Environ. Sci. Technol. 49 (2015) 6599–6607.

[14] C.J. Weschler, H.C. Shields, Production of the hydroxyl radical in indoor air, Environ. Sci. Technol. 30 (1996) 3250–3258.
[15] T. Wainman, C.J. Weschler, P.J. Lioy, J. Zhang, Effects of surface type and relative humidity on the production and concentration of nitrous acid in a model indoor environment, Environ. Sci. Technol. 35 (2001) 2200–2206.
[16] C.J. Weschler, Chemical reactions among indoor pollutants: what we've learned in the new millennium, Indoor Air 14 (Suppl. 7) (2004) 184–194.
[17] W.W. Nazaroff, C.J. Weschler, R.L. Corsi, Indoor air chemistry and physics, Atmos. Environ. 37 (2003) 5451–5453.
[18] E. Gómez Alvarez, D. Amedro, A. Charbel, S. Gligorovski, C. Schoemaecker, C. Fittschen, J.-F. Doussin, H. Wortham, Unexpectedly high indoor hydroxyl radical concentrations associated with nitrous acid, Proc. Natl. Acad. Sci. 110 (2013) 13294–13299.
[19] S. Gligorovski, Nitrous acid (HONO): an emerging indoor pollutant, J. Photochem. Photobiol. A: Chem. 314 (2016) 1–5.
[20] K.A. Ramazan, D. Syomin, B.J. Finlayson-Pitts, The photochemical production of HONO during the heterogeneous hydrolysis of NO_2, Phys. Chem. Chem. Phys. 6 (2004) 3836.
[21] N. Carslaw, A new detailed chemical model for indoor air pollution, Atmos. Environ. 41 (2007) 1164–1179.
[22] B.J. Finlayson-Pitts, L.M. Wingen, A.L. Sumner, D. Syomin, K.A. Ramazan, The heterogeneous hydrolysis of NO_2 in laboratory systems and in outdoor and indoor atmospheres: an integrated mechanism, Phys. Chem. Chem. Phys. 5 (2003) 223–242.
[23] E. Gómez Alvarez, M. Sörgel, S. Gligorovski, S. Bassil, V. Bartolomei, B. Coulomb, C. Zetzsch, H. Wortham, Light-induced nitrous acid (HONO) production from NO_2 heterogeneous reactions on household chemicals, Atmos. Environ. 95 (2014) 391–399.
[24] V. Bartolomei, M. Sörgel, S. Gligorovski, E.G. Alvarez, A. Gandolfo, R. Strekowski, E. Quivet, A. Held, C. Zetzsch, H. Wortham, Formation of indoor nitrous acid (HONO) by light-induced NO_2 heterogeneous reactions with white wall paint, Environ. Sci. Pollut. Res. 21 (2014) 9259–9269.
[25] WHO, Air Quality Guidelines for Particulate Matter, Ozone, Nitrogen Dioxide and Sulfur Dioxide: Global Update 2005: Summary of Risk Assessment, 2006.
[26] J.J. Kim, S. Smorodinsky, M. Lipsett, B.C. Singer, A.T. Hodgson, B. Ostro, Traffic-related air pollution near busy roads, Am. J. Respir. Crit. Care Med. 170 (2004) 520–526.
[27] E.A. Harwood, P.B. Hopkins, S.T. Sigurdsson, Chemical synthesis of cross-link lesions found in nitrous acid treated DNA: a general method for the preparation of N_2-substituted 2′-deoxyguanosines, J. Org. Chem. 65 (2000) 2959–2964.
[28] M. Sleiman, L.A. Gundel, J.F. Pankow, P. Jacob, B.C. Singer, H. Destaillats, Formation of carcinogens indoors by surface-mediated reactions of nicotine with nitrous acid, leading to potential thirdhand smoke hazards, Proc. Natl. Acad. Sci. U. S. A. 107 (2010) 6576–6581.
[29] Y. Huang, S.S.H. Ho, R. Niu, L. Xu, Y. Lu, J. Cao, S. Lee, Removal of indoor volatile organic compounds via photocatalytic oxidation: a short review and prospect, Molecules 21 (2016).
[30] F. Petronella, A. Truppi, C. Ingrosso, T. Placido, M. Striccoli, M.L. Curri, A. Agostiano, R. Comparelli, Nanocomposite materials for photocatalytic degradation of pollutants, Catal. Today 281 (2017) 85–100.
[31] J.M. Langridge, R.J. Gustafsson, P.T. Griffiths, R.A. Cox, R.M. Lambert, R.L. Jones, Solar driven nitrous acid formation on building material surfaces containing titanium dioxide: a concern for air quality in urban areas? Atmos. Environ. 43 (2009) 5128–5131.
[32] S. Laufs, G. Burgeth, W. Duttlinger, R. Kurtenbach, M. Maban, C. Thomas, P. Wiesen, J. Kleffmann, Conversion of nitrogen oxides on commercial photocatalytic dispersion paints, Atmos. Environ. 44 (2010) 2341–2349.
[33] A. Gandolfo, V. Bartolomei, E. Gomez Alvarez, S. Tlili, S. Gligorovski, J. Kleffmann, H. Wortham, The effectiveness of indoor photocatalytic paints on NOx and HONO levels, Appl. Catal. B: Environ. 166–167 (2015) 84–90.
[34] K. Stemmler, M. Ammann, C. Donders, J. Kleffmann, C. George, Photosensitized reduction of nitrogen dioxide on humic acid as a source of nitrous acid, Nature 440 (2006) 195–198.
[35] M. Ndour, B. D'Anna, C. George, O. Ka, Y. Balkanski, J. Kleffmann, K. Stemmler, M. Ammann, Photoenhanced uptake of NO_2 on mineral dust: laboratory experiments and model simulations, Geophys. Res. Lett. 35 (2008).
[36] A. El Zein, Y. Bedjanian, Interaction of NO_2 with TiO_2 surface under UV irradiation: measurements of the uptake coefficient, Atmos. Chem. Phys. 12 (2012) 1013–1020.
[37] L. Wu, S. Tong, M. Ge, Heterogeneous reaction of NO_2 on Al_2O_3: the effect of temperature on the nitrite and nitrate formation, J. Phys. Chem. A 117 (2013) 4937–4944.
[38] A. Gandolfo, V. Gligorovski, V. Bartolomei, S. Tlili, E. Gómez Alvarez, H. Wortham, J. Kleffmann, S. Gligorovski, Spectrally resolved actinic flux and photolysis frequencies of key species within an indoor environment, Build. Environ. 109 (2016) 50–57.
[39] D. Grosjean, J. Harrison, Response of chemiluminescence NOx analyzers and ultraviolet ozone analyzers to organic air pollutants, Environ. Sci. Technol. 19 (1985) 862–865.
[40] M. Steinbacher, C. Zellweger, B. Schwarzenbach, S. Bugmann, B. Buchmann, C. Ordóñez, A.S.H. Prevot, C. Hueglin, Nitrogen oxide measurements at rural sites in Switzerland: bias of conventional measurement techniques, J. Geophys. Res. 112 (2007) D11307.
[41] A.M. Winer, J.W. Peters, J.P. Smith, J.N. Pitts, Response of commercial chemiluminescent nitric oxide–nitrogen dioxide analyzers to other nitrogen-containing compounds, Environ. Sci. Technol. 8 (1974) 1118–1121.
[42] J. Heland, J. Kleffmann, R. Kurtenbach, P. Wiesen, A new instrument to measure gaseous nitrous acid (HONO) in the atmosphere, Environ. Sci. Technol. 35 (2001) 3207–3212.
[43] J. Kleffmann, J. Heland, R. Kurtenbach, J. Lorzer, P. Wiesen, A new instrument (LOPAP) for the detection of nitrous acid (HONO), Environ. Sci. Pollut. Res. 9 (4) (2002) 48–54.
[44] J. Kleffmann, P. Wiesen, Technical note: quantification of interferences of wet chemical HONO LOPAP measurements under simulated polar conditions, Atmos. Chem. Phys. 8 (2008) 6813–6822.
[45] S. Gligorovski, C.J. Weschler, The oxidative capacity of indoor atmospheres, Environ. Sci. Technol. 47 (2013) 13905–13906.
[46] M.P. McGrath, F.S. Rowland, Determination of the barriers to internal rotation in ONOOX (X = H, Cl) and characterization of the minimun energy conformers, J. Phys. Chem. 98 (1994) 1061–1067.
[47] R. Sumathi, S.D. Peyerimhoff, An ab initio molecular orbital study of the potential energy surface of the HO_2 + NO reaction, J. Chem. Phys. 107 (1997).
[48] J.D. Spengler, J.F. McCarthy, J.M. Samet, Indoor Air Quality Handbook, McGraw-Hill, New York, 2001.
[49] S.A. Nizkorodov, P.O. Wennberg, First spectroscopic observation of gas-phase HOONO, J. Phys. Chem. A 106 (2002) 855–859.
[50] O. Abida, L.H. Mielke, H.D. Osthoff, Observation of gas-phase peroxynitrous and peroxynitric acid during the photolysis of nitrate in acidified frozen solutions, Chem. Phys. Lett. 511 (2011) 187–192.
[51] D.M. Golden, J.R. Barker, L.L. Lohr, Master equation models for the pressure- and temperature-dependent reactions $HO + NO_2 \rightarrow HONO_2$ and $HO + NO_2 \rightarrow HOONO$, J. Phys. Chem. A 107 (2003) 11057–11071.
[52] J.M. Herrmann, Heterogeneous photocatalysis: state of the art and present applications, Top. Catal. 34 (2005) 49–65.
[53] A.M. Elabsy, Effect of temperature on the binding energy of a confined impurity to a spherical semiconductor quantum dot, Phys. Scr. 59 (1999) 328–330.
[54] G. da Silva, E.M. Kennedy, B.Z. Dlugogorski, Ab initio procedure for aqueous-phase pKa calculation: the acidity of nitrous acid, J. Phys. Chem. A 110 (2006) 11371–11376.
[55] H. Su, Y. Cheng, R. Oswald, T. Behrendt, I. Trebs, F.X. Meixner, M.O. Andreae, P. Cheng, Y. Zhang, U. Pöschl, Soil nitrite as a source of atmospheric HONO and OH radicals, Science 333 (2011) 1616–1618.
[56] L.A. Wallace, S.J. Emmerich, C. Howard-Reed, Continuous measurements of air change rates in an occupied house for 1 year: the effect of temperature, wind, fans, and windows, J. Expo. Anal. Environ. Epidemiol. 12 (2002) 296–306.
[57] S. Gligorovski, H. Wortham, J. Kleffmann, The hydroxyl radical (OH) in indoor air: sources and implications, Atmos. Environ. 99 (2014) 568–570.
[58] S.K. Brown, M.R. Sim, M.J. Abramson, C.N. Gray, Concentrations of volatile organic compounds in indoor air – a review, Indoor Air 4 (1994) 123–134.
[59] R. Atkinson, D. Hasegawa, S.M. Aschmann, Rate constants for the gas-phase reactions of O_3 with a series of monoterpenes and related compounds at 296 ± 2 K, Int. J. Chem. Kinet. 22 (1990) 871–887.
[60] C.R. Greene, R. Atkinson, Rate constants for the gas-phase reactions of O_3 with a series of alkenes at 296 ± 2 K, Int. J. Chem. Kinet. 24 (1992) 803–811.
[61] Royal Society, Ground-level Ozone in the 21st Century: Future Trends, Impacts and Policy Implications, 2008.
[62] C.J. Weschler, Ozone in indoor environments: concentration and chemistry, Indoor Air 10 (2000) 269–288.
[63] J.D. Lee, L.K. Whalley, D.E. Heard, D. Stone, R.E. Dunmore, J.F. Hamilton, D.E. Young, J.D. Allan, S. Laufs, J. Kleffmann, Detailed budget analysis of HONO in central London reveals a missing daytime source, Atmos. Chem. Phys. 16 (2016) 2747–2764.
[64] X. Ren, W.H. Brune, C.A. Cantrell, G.D. Edwards, T. Shirley, A.R. Metcalf, R.L. Lesher, Hydroxyl and peroxy radical chemistry in a rural area of central pennsylvania: observations and model comparisons, J. Atmos. Chem. 52 (2005) 231–257.